

DOI:10.1002/ejic.201301515

# Two Tetranuclear Copper(II) Complexes with Open Cubane-Like $\text{Cu}_4\text{O}_4$ Core Framework and Ferromagnetic Exchange Interactions between Copper(II) Ions: Structure, Magnetic Properties, and Density Functional Study

Elif Gungor,<sup>\*[a]</sup> Hulya Kara,<sup>[a]</sup> Enrique Colacio,<sup>\*[b]</sup> and Antonio J. Mota<sup>[b]</sup>

**Keywords:** Copper / Schiff bases / Magnetic properties / Density functional calculations

Two alkoxo-bridged copper(II) tridentate Schiff base complexes  $[\{\text{Cu}(\text{H}_2\text{L}1)\}_4]$  (**1**) [ $\text{H}_2\text{L}1 = N$ -(2-hydroxyethyl)-3,5-di-*tert*-butylsalicylaldehyde] and  $[\{\text{Cu}(\text{H}_2\text{L}2)\}_4]$  (**2**) [ $\text{H}_2\text{L}2 = N$ -(2-hydroxyethyl)-4-methoxysalicylaldehyde] have been synthesized and structurally and magnetically characterized. X-ray diffraction studies show that **1** and **2** are tetranuclear alkoxo-bridged copper(II) complexes that contain a rather distorted  $\text{Cu}_4\text{O}_4$  cubane core of 4+2 type (four short and two long Cu...Cu distances). The coordination of each copper ion can be described as a distorted square pyramid with one nitrogen and four oxygen atoms from three ligands. Variable-temperature magnetic susceptibility measurements on the two tetra-

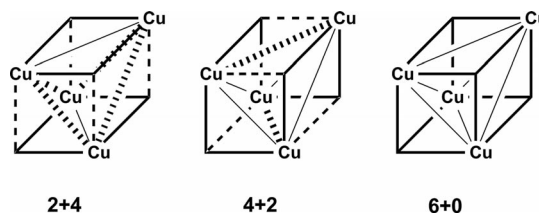
nuclear complexes **1** and **2** in the range 2–300 K indicate ferromagnetic exchange coupling between copper(II) centers. The magnetic susceptibility data were analyzed by using a simple two- $J$  model with  $J'$  and  $J''$  representing the magnetic exchange couplings through the short and long Cu...Cu exchange pathways, respectively. The  $J$  values were as follows:  $J' = +28.7 \text{ cm}^{-1}$  and  $J'' = +7.8 \text{ cm}^{-1}$  for **1**, and  $J' = +39.8 \text{ cm}^{-1}$  and  $J'' = +10.2 \text{ cm}^{-1}$  for **2**. The sign and magnitude of the exchange coupling constants were justified on the basis of the structural geometric factors of the bridging  $\text{Cu}(\text{O})_2\text{Cu}$  fragments, the overlap of the magnetic orbitals, and DFT calculations.

## Introduction

Polynuclear copper(II) complexes have attracted much attention during recent decades owing to their interesting architectures and potential applications in fields such as coordination polymers,<sup>[1]</sup> magnetochemistry,<sup>[2]</sup> bioinorganic chemistry,<sup>[3]</sup> and catalysis.<sup>[4]</sup> Among them, cubane-like  $\text{Cu}_4\text{O}_4$  complexes that contain hydroxo, alkoxo, or phenoxo bridges are relatively common<sup>[5]</sup> and have been studied from a magneto-structural point of view with experimental and theoretical approaches.<sup>[6]</sup> Two classifications of  $\text{Cu}_4\text{O}_4$  cubane-like complexes have been proposed on the basis of their structural features. Chronologically, the first one was suggested by Mergehenn and Haase,<sup>[7]</sup> who classified these compounds into two types (I and II), depending on the

length of the Cu–O bonds within the cubane unit. Thus,  $\text{Cu}_4\text{O}_4$  cubane complexes with four long Cu–O distances between two dinuclear subunits are classified as type I, whereas those with long Cu–O distances within each dinuclear subunit are classified as type II.

The second one was proposed by Alvarez et al.<sup>[6]</sup> and uses the Cu...Cu distances within the cubane unit to classify the  $\text{Cu}_4\text{O}_4$  complexes into three types (see Scheme 1): (i) 2+4, which is equivalent to type I and has two short and four long Cu...Cu distances, (ii) 4+2, which contains four short and two long Cu...Cu distances and when the symmetry is  $S_4$  would be equivalent to type II, and (iii) 6+0, which contains six similar Cu...Cu distances.



Scheme 1. Structural types of  $\text{Cu}_4\text{O}_4$  cubane complexes classified according to the Cu...Cu distances. Short Cu...Cu distances (solid lines), long Cu...Cu distances (hashed lines), short Cu–O bond lengths (bold lines), and long Cu–O distances (dashed lines).

[a] Department of Physics, Faculty of Science and Art, Balıkesir University, 10145 Balıkesir, Turkey  
E-mail: egungor@balikesir.edu.tr  
<http://w3.balikesir.edu.tr/~egungor>  
<http://w3.balikesir.edu.tr/~hkara>

[b] Departamento de Química Inorgánica, Universidad de Granada, 18071 Granada, Spain  
E-mail: ecolacio@ugr.es  
<http://inorganica.ugr.es>  
<http://www.ugr.es/local/mota>

Supporting information for this article is available on the WWW under <http://dx.doi.org/10.1002/ejic.201301515>.

Although the analysis of the magneto-structural data for  $\text{Cu}_4\text{O}_4$  cubane complexes has allowed the understanding of the main structural factors that govern the magnetic exchange coupling in this type of system,<sup>[6a]</sup> no simple magneto-structural correlations could be established for them.

Moreover, there is a contradictory result for 4+2 type complexes because the sign of the experimental magnetic exchange coupling through the long  $\text{Cu}\cdots\text{Cu}$  pathways is generally opposite to that obtained from DFT calculations.<sup>[6a]</sup> Therefore, more examples of this type of complex are needed, not only to clarify this point but also to support previous results. In connection with this, we are reporting here the synthesis, crystal structure, magnetic properties, and DFT calculations of two new examples of ferromagnetically coupled tetranuclear copper(II) complexes with open cubane-like  $\text{Cu}_4\text{O}_4$  core framework. Interestingly, for these complexes, the sign and magnitude of the experimental magnetic coupling constants agree well with those predicted from DFT calculations for 4+2  $\text{Cu}_4\text{O}_4$ -type complexes.

## Results and Discussion

### Crystal Structure Description of 1 and 2

The structures of **1** and **2** are illustrated in Figures 1 and 2. The crystallographic data, conditions used for the intensity data collection, and some features of the structure refinement are listed in Table 1. Selected bond lengths and angles are listed in Table 2.

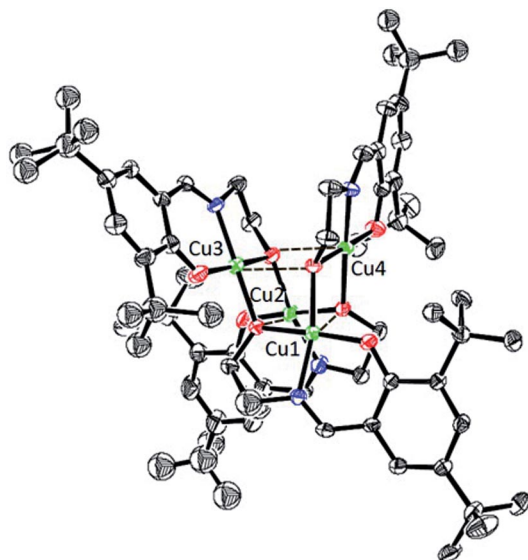


Figure 1. ORTEP drawing of complex **1** with atom labeling. Thermal ellipsoids have been drawn at 30% probability level (hydrogen atoms are omitted for clarity).

The crystal structure of **1** has been reported previously at room temperature.<sup>[8]</sup> We report here a redetermination of **1** in detail. The precision of the unit-cell dimensions was improved by an order of magnitude. The unit-cell volume decreased by approximately  $771.9 \text{ \AA}^3$  for **1**.<sup>[8]</sup>

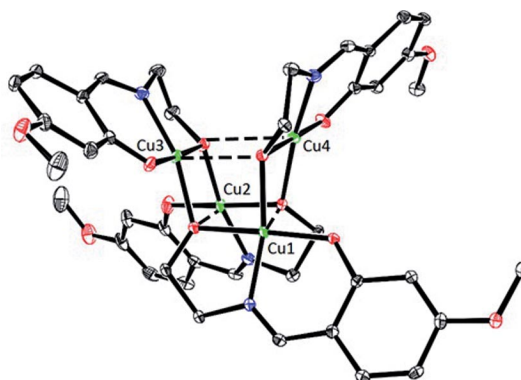


Figure 2. ORTEP drawing of complex **2** with atom labeling. Thermal ellipsoids have been drawn at 30% probability level (hydrogen atoms are omitted for clarity).

Table 1. Crystal data and structure refinement compound **1** and **2**.

	<b>1</b>	<b>2</b>
Chemical formula	$\text{C}_{68}\text{H}_{100}\text{Cu}_4\text{N}_4\text{O}_8$	$\text{C}_{40}\text{H}_{44}\text{Cu}_4\text{N}_4\text{O}_{12}$
$M_r$	1355.68	1026.95
$T$	293(2)	100(2)
Crystal system	monoclinic	triclinic
Space group	$P2_1/c$	$P\bar{1}$
$a$ [Å]	24.6826(7)	11.5022(4)
$b$ [Å]	15.1397(6)	11.9664(4)
$c$ [Å]	19.6794(6)	16.1999(6)
$\alpha$ [°]	90	81.022(2)
$\beta$ [°]	95.160(3)	71.223(2)
$\gamma$ [°]	90	72.461(2)
$V$ [Å <sup>3</sup> ]	7324.1(4)	2008.63(13)
$Z$	4	2
$\rho_{\text{calcd.}}$ [g cm <sup>-3</sup> ]	1.230	1.698
$\mu$ [mm <sup>-1</sup> ]	1.196	2.158
Reflections collected	33530	34111
Independent reflections	17010	14193
Data/parameters	5992/688	9250/545
GoF on $F^2$	0.9	1.02
$R$ indices [ $I > 2\sigma(I)$ ]	$R_1 = 0.0715,$ $wR_2 = 0.2148$	$R_1 = 0.0325,$ $wR_2 = 0.0755$

In the main structural unit of **1** and **2**, it is seen that the  $\text{Cu}_4\text{O}_4$  core consists of four alkoxo-bridged copper atoms to give an approximately cubic array of alternating copper and oxygen atoms that occupy the corners of the cube. All copper(II) centers are pentacoordinate with an  $\text{NO}_4$  donor set from the Schiff base ligands. For a pentacoordinate metal center, the distortion of the coordination environment from trigonal bipyramidal (TBP) to square pyramidal (SP) can be evaluated by the Addison distortion index ( $\tau$ ) defined as  $\tau = (a - \beta)/60$ , in which  $a$  and  $\beta$  are the two largest coordination angles, and  $\tau = 0$  for perfect SP and 1 for ideal TBP.<sup>[23]</sup> The structural distortion indexes of  $\text{Cu}_1$ ,  $\text{Cu}_2$ ,  $\text{Cu}_3$ , and  $\text{Cu}_4$  atoms were found to be  $\tau_{\text{Cu}_1} = 0.0016$ ,  $\tau_{\text{Cu}_2} = 0.024$ ,  $\tau_{\text{Cu}_3} = 0.027$ , and  $\tau_{\text{Cu}_4} = 0.016$  for **1**, and  $\tau_{\text{Cu}_1} = 0.024$ ,  $\tau_{\text{Cu}_2} = 0.027$ ,  $\tau_{\text{Cu}_3} = 0.015$ , and  $\tau_{\text{Cu}_4} = 0.024$  for **2**, respectively. Therefore, the coordination polyhedron of each copper(II) center is best described as distorted square pyramidal. The slight distortion in the basal plane may be

Table 2. Some selected bond lengths [Å] and angles [°] for **1** and **2**.

	<b>1</b>	<b>2</b>
Cu1–O1	1.868(4)	1.913(1)
Cu1–O2	1.953(4)	1.988(1)
Cu1–O5	1.939(4)	1.963(2)
Cu1–O7	2.478(4)	2.323(1)
Cu1–N1	1.907(4)	1.932(2)
Cu2–O2	1.960(4)	1.947(2)
Cu2–O3	1.905(4)	1.902(1)
Cu2–O4	1.960(4)	1.966(1)
Cu2–O5	2.401(4)	2.575(1)
Cu2–N2	1.914(7)	1.938(3)
Cu3–O5	1.968(4)	1.966(1)
Cu3–O6	1.872(4)	1.895(1)
Cu3–O7	1.967(4)	1.999(2)
Cu3–O4	2.470(4)	2.282(1)
Cu3–N3	1.925(6)	1.933(2)
Cu4–O4	1.938(4)	1.946(2)
Cu4–O7	1.960(4)	1.956(1)
Cu4–O8	1.873(4)	1.890(1)
Cu4–O2	2.506(4)	2.600(1)
Cu4–N4	1.914(6)	1.928(2)
Cu1–O2–Cu2	105.450(1)	109.500(9)
Cu1–O2–Cu4	96.440(1)	94.080(7)
Cu1–O5–Cu2	91.005(1)	89.130(7)
Cu1–O5–Cu3	106.100(1)	102.460(8)
Cu1–O7–Cu3	88.450(1)	89.950(7)
Cu1–O7–Cu4	97.160(1)	104.150(7)
Cu2–O2–Cu4	88.890(1)	87.310(7)
Cu2–O4–Cu3	98.730(1)	104.890(8)
Cu2–O4–Cu4	107.920(1)	108.430(9)
Cu2–O5–Cu3	100.840(1)	95.020(7)
Cu3–O4–Cu4	91.310(1)	92.260(8)
Cu3–O7–Cu4	107.800(2)	101.230(9)

attributed to the strain imposed by the ligand to the metal center during coordination.

Cu··Cu distances on different cubic faces of **1** and **2** are also different; they vary from 3.058 to 3.378 Å, which are quite comparable to those values of the similar tetramer copper(II) complexes reported in the literature.<sup>[5d,6b,6c]</sup> The basal plane of the square pyramid is constructed by the phenolate oxygen atom, the imine nitrogen atom, and two  $\mu_3$ -alkoxide oxygen atoms, whereas the apical position is occupied by another  $\mu_3$ -alkoxide oxygen atom. Cu1, Cu2, Cu3, and Cu4 deviate from the NO<sub>3</sub> basal planes by 0.062, 0.056, 0.060, and 0.069 Å for **1**, and 0.142, 0.105, 0.108, and 0.091 Å for **2**, respectively, towards the apical ligand atom.

The basal Cu–O and Cu–N bond lengths of **1** and **2** are in the range 1.868(4)–1.999(2) Å and 1.907(4)–1.938(3) Å, respectively, which lie well within the range of reported values for corresponding bond lengths of other copper(II) tetranuclear cubane clusters.<sup>[5d,5s]</sup> The axial Cu–O bond lengths are in the range 2.401(4)–2.506(4) Å for **1** and 2.282(18)–2.600(17) Å for **2**. The elongated of the Cu–O axial bonds can be explained by Jahn–Teller distortions, which is typical for copper(II) d<sup>9</sup>.

Finally, before proceeding to the magnetic characterization, we note that the powder patterns for bulk microcrystalline samples of **1** and **2** were consistent with the exclusive presence of the phase identified in the single-crystal experiment (Figures S1 and S2 in the Supporting Information).

## Magnetic Properties of Complexes **1** and **2**

The temperature dependence of  $\chi_M T$  ( $\chi_M$  is the molar magnetic susceptibility per Cu<sub>4</sub> unit) for **1** and **2** in the range 300–2 K and at an applied field of 1000 Oe is shown in Figure 3.

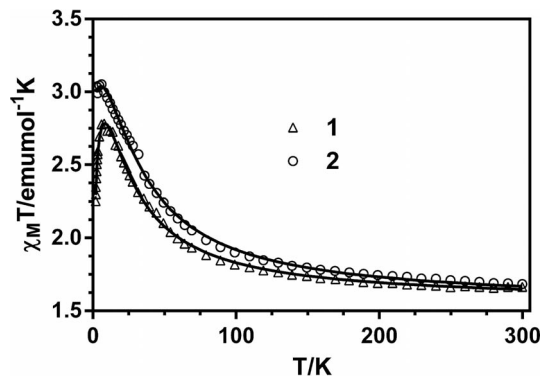


Figure 3. Temperature dependence of  $\chi_M T$  for **1** and **2**.

The  $\chi_M T$  value at room temperature for **1** and **2** (1.66 and 1.68 cm<sup>3</sup> mol<sup>-1</sup> K, respectively) is slightly higher than that expected for four uncoupled Cu<sup>2+</sup> ions ( $S = 1/2$ ) with  $g = 2.0$  (1.50 cm<sup>3</sup> mol<sup>-1</sup> K). When the temperature is lowered,  $\chi_M T$  steadily increases to reach a maximum at 8 K (2.78 cm<sup>3</sup> mol<sup>-1</sup> K) for **1** and at 6 K (2.78 cm<sup>3</sup> mol<sup>-1</sup> K) for **2**, respectively. Below the temperature of the maximum, the  $\chi_M T$  value decreases to 2 K to reach values of 2.25 and 3.01 cm<sup>3</sup> mol<sup>-1</sup> K for **1** and **2**, respectively.

This behavior is due to a significant intratetranuclear ferromagnetic coupling between the copper(II) ions, which leads to a  $S = 2$  ground state. The decrease in  $\chi_M T$  at low temperatures suggests the existence of zero-field splitting effects (ZFS) of the  $S = 2$  ground state and/or intermolecular antiferromagnetic interactions.

Complexes **1** and **2**, which exhibit an open cubane-like Cu<sub>4</sub>O<sub>4</sub> structure with four short and two long Cu··Cu distances (see Figure 4), belong to the 4+2 type. A close inspection of the structure of **1** and **2** reveals that their respective 4+2 Cu<sub>4</sub>O<sub>4</sub> cubane units are rather asymmetric, so that six different  $J$  values should be taken into account to analyze the magnetic data. However, to avoid overparametrization, we have assumed that the exchange coupling constants between the copper(II) ions that involve short Cu··Cu distances are equivalent and described by  $J'$ , whereas those that involve long Cu··Cu distances are described by  $J''$  (see Figure 4).

In keeping with the above considerations, the experimental magnetic susceptibility data for **1** and **2** were analyzed by using the following two- $J$  isotropic Hamiltonian [Equation (1)].

$$H = -J'(S_{Cu1}S_{Cu2} + S_{Cu1}S_{Cu3} + S_{Cu2}S_{Cu4} + S_{Cu3}S_{Cu4}) - J''(S_{Cu1}S_{Cu4} + S_{Cu2}S_{Cu3}) \quad (1)$$

This model implies that exchange interactions between the Cu<sup>II</sup> ions that belong to the short and long Cu··Cu distances are averaged in each case. A  $zJ$  parameter was in-

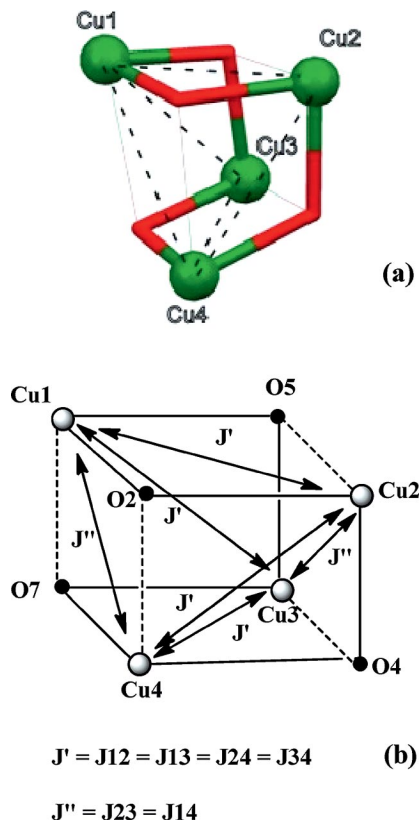


Figure 4. (a) A view of the  $\text{Cu}_4\text{O}_4$  core of **1** and **2** with (b) the exchange coupling pattern.

cluded to account for intercube magnetic interactions by using the molecular-field approximation, and an average  $g$  value was assumed for the whole  $\text{Cu}_4\text{O}_4$  unit. The Hamiltonian was numerically diagonalized using the MAGPACK program.<sup>[24]</sup> The best-fit parameters were as follows:  $J' =$

$+28.7 \text{ cm}^{-1}$ ,  $J'' = +7.8 \text{ cm}^{-1}$ ,  $g = 2.036$ , and  $zJ = -0.25 \text{ cm}^{-1}$  for **1** and  $J' = +39.8 \text{ cm}^{-1}$ ,  $J'' = +10.2 \text{ cm}^{-1}$ ,  $g = 2.025$ , and  $zJ = -0.02 \text{ cm}^{-1}$  for **2**. It is worth mentioning that intermolecular interactions and the ZFS effects of the ground state have a similar effect on the magnetic properties at low temperature and consequently are strongly correlated. Therefore, the extracted  $zJ$  values can be considered the upper limit for the intercube interactions. The experimental  $J'$  and  $J''$  coupling constants reported for 4+2  $\text{Cu}_4\text{O}_4$  cubane-like complexes (Table 3) are ferromagnetic and antiferromagnetic, respectively, with only one exception along each of the series of coupling constants.

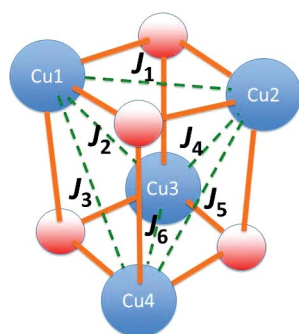
Although the sign of  $J''$  determined for **1** and **2** seems to be in contradiction with the reported experimental values, DFT calculations carried out by Alvarez et al. on models of 4+2 systems agree with our results as they always found weakly ferromagnetic  $J''$  coupling constants, which were practically independent of the geometry. To support the experimental values of  $J'$  and  $J''$  for compounds **1** and **2** and to calculate the “remaining” possible  $J$  values for these compounds (as indicated elsewhere, the  $\text{Cu}_4\text{O}_4$  cubane unit is rather asymmetric, with six different exchange pathways), DFT calculations were carried out on the X-ray structures as found in the solid state. The calculated  $J$  values for **1** and **2** are given in Scheme 2.

The values of  $J'_{\text{mean}}$  (average value of the calculated  $J_1$ ,  $J_2$ ,  $J_5$ , and  $J_6$  calculated exchange coupling constant) and  $J''_{\text{mean}}$  (average value of the calculated  $J_3$  and  $J_4$ ) are respectively  $+30.2$  and  $+4.45 \text{ cm}^{-1}$  for **1** and  $+36$  and  $+6.8 \text{ cm}^{-1}$  for **2** (see Scheme 2). The sign and relative magnitude of these interactions are in good accord with the experimental results, which indicate that  $J'$  and  $J''$  are both ferromagnetic and larger for **2** than for **1**. Moreover, as expected,  $J''$  is weakly ferromagnetic and much weaker than  $J'$ .

Table 3. Structural and magnetic data for **1**, **2**, and a series of related compounds.

Complex	Class	Cu...Cu [Å]	Cu–O [Å]	Cu–O–Cu [°]	$J$ [ $\text{cm}^{-1}$ ]	Ref.
$\{\text{Cu}(\text{H}_2\text{L}1)\}_4$	4+2	3.114–3.378	1.868–1.968	88.45–107.97	+28.7, +7.8	this work
$\{\text{Cu}(\text{H}_2\text{L}2)\}_4$	4+2	3.058–3.384	1.890–1.999	89.95–109.50	+39.8, +10.2	this work
$[\text{Cu}_4(\text{hsae})_4] \cdot 2\text{H}_2\text{O} \cdot 4\text{MeCN}^{[a]}$	4+2	3.108–3.615	1.930–2.00	85.80–106.10	+72, –35.2	[5m]
$[\text{Cu}_4(\text{dpd-H})_4(\text{ClO}_4)_2(\text{H}_2\text{O})_2]^{[b]}$	4+2	3.129–3.307	1.934–2.010	86.20–112.10	–6.40, –10.90	[5o]
$[\text{Cu}_4(\text{L}^1)_4] \cdot \text{Na} \cdot \text{ClO}_4^{[c]}$	4+2	3.229–3.486	1.934–1.971	86.20–112.10	+13.60, –34.90	[5v]
$[\text{Cu}_4(\text{MeCOCHCMe}=\text{NCH}_2\text{CHO})_4]$	4+2	3.021–3.492	1.920–1.970	87.30–109.80	+41, –19.80	[5n]
$[\text{Cu}_4(\text{L}^2)_2(\text{OMe})_2] \cdot 2\text{H}_2\text{O} \cdot \text{THF}^{[d]}$	4+2	3.070–3.419	1.950–1.990	88.30–104.00	+33.30, –15.60	[5s]
$[\text{Cu}_4(\text{L}^2)_2(\text{OH})_2] \cdot 6\text{H}_2\text{O}^{[d]}$	4+2	3.103–3.458	1.930–1.970	88.80–105.80	+14.70, –18.40	[5s]
$[\text{Cu}_4(\text{L}^3)_4]^{[e]}$	4+2	3.114–3.415	1.900–1.970	88.80–107.70	+15.20, –9.40	[5u]
$[\text{Cu}_4(\text{L}^4)_4] \cdot 9\text{MeOH}^{[f]}$	4+2	3.124–3.512	1.960–2.00	88.80–104.40	+57, –14	[5t]
$[\text{Cu}_4\text{Br}_4(\text{CH}_2\text{CH}_2\text{NEt}_2)_4] \cdot 4\text{CCl}_4$	4+2	3.176–3.523	1.920–1.980	88.80–108.80	+80, –9	[5j]
$[\text{Cu}_4(\text{L}^5)_4] \cdot 4\text{H}_2\text{O}^{[g]}$	4+2	2.961–3.333	1.894–1.907	97.10–101.0	+2.16, –103.40	[5b]
$[\text{Cu}_4(\text{NH}_3)_4(\text{HL}^6)_4][\text{CdBr}_4]\text{Br}_2 \cdot 3\text{dmf} \cdot \text{H}_2\text{O}^{[h]}$	4+2	3.127–3.503	1.928–2.099	100.0–107.0	+1, –65	[5y]
$[\text{Cu}_4(\text{L}^7)_4] \cdot 5\text{CH}_3\text{OH} \cdot \text{H}_2\text{O}^{[i]}$	4+2	3.095–3.413	1.886–1.984	102.00–109.40	+33, –15.80	[5d]
$[\text{Cu}_4(\text{hsae})_4] \cdot 2\text{H}_2\text{O} \cdot 4\text{CH}_3\text{CN}^{[a]}$	4+2	3.108–3.615	1.894–2.000	104.80–106.10	+36, –17.60	[5k]
$[\text{Cu}_4(\text{hpda})_4](\text{ClO}_4)_4 \cdot \text{H}_2\text{O}^{[l]}$	4+2	3.150–3.410	1.920–1.990	108.00–110.10	+89.80, –32.60	[5c]
$[\text{Cu}_4(\text{HL}^8)_4]\text{DMF}^{[k]}$	4+2	3.293–3.315	1.967–1.980	113.06	–37.46, –2.45	[5z]

[a]  $\text{H}_2\text{hsae}$ : 2-(4-hydroxysalicylideneamino)-1-ethanol. [b] dpd-H: the hydrated *gem*-diol form  $[(\text{C}_5\text{H}_4\text{N})_2\text{CO}(\text{OH})]$ , dpd-H) of di-2-pyridylketone. [c]  $\text{H}_2\text{L}^1$ :  $N'$ -(2-hydroxy-3-methoxybenzylidene)benzohydrazide. [d]  $\text{H}_2\text{L}^2$ :  $N,N'$ -(2-hydroxypropane-1,3-diyl)bis(salicylaldehyde). [e]  $\text{H}_2\text{L}^3$ : ethyl 2-[ $N'$ -(2-hydroxycyclohexyl)aminomethylene]-3-oxobutanoate. [f]  $\text{H}_2\text{L}^4$ : Schiff base of pyridoxal and 2-amino-1-phenylpropan-1-ol. [g]  $\text{H}_2\text{L}^5$ : 2-(3-methoxysalicylideneamino)benzyl alcohol. [h]  $\text{H}_2\text{L}^6$ : Schiff base of cadmium oxide in the air-exposed solution of ammonium bromide and diethanolamine in dimethylformamide (dmf). [i]  $\text{H}_2\text{L}^7$ : 2-(5-fluorosalicylideneamino)ethanol. [j]  $\text{H}_2\text{hpda}$ :  $N$ -(2-hydroxyethyl)-1,3-propanediamine. [k]  $\text{H}_3\text{L}^8$ :  $N'$ -(2-hydroxy-3-methoxybenzylidene)-2-hydroxybenzohydrazide.



1	2
$d_{\text{Cu1-Cu2}} = 3.114 \text{ \AA}$	$d_{\text{Cu1-Cu2}} = 3.214 \text{ \AA}$
$d_{\text{Cu3-Cu4}} = 3.174 \text{ \AA}$	$d_{\text{Cu3-Cu4}} = 3.058 \text{ \AA}$
$J$ in $\text{cm}^{-1}$	$J$ in $\text{cm}^{-1}$
$J_1 = +38.6$	$J_1 = +19.3$
$J_2 = +35.5$	$J_2 = +55.1$
$J_3 = +3.5$	$J_3 = +6.6$
$J_4 = +5.4$	$J_4 = +7.0$
$J_5 = +25.2$	$J_5 = +22.8$
$J_6 = +21.6$	$J_6 = +46.8$
$J'_{\text{mean}} = +30.2$	$J'_{\text{mean}} = +36.0$
$J''_{\text{mean}} = +4.45$	$J''_{\text{mean}} = +6.8$

Scheme 2. Calculated  $J_i$  values inside the  $\text{Cu}_4\text{O}_4$  unit as found in the crystal structures of complexes **1** and **2**.

It should be noted at this point that both experimental<sup>[25]</sup> and theoretical<sup>[25h,25i,6a,26]</sup> studies have shown that the major factor that controls the magnetic exchange interaction in hydroxo- and alkoxo-bridged polynuclear copper(II) complexes is the value of the Cu–O–Cu angle ( $\theta$ ), and an almost linear variation of  $J$  with  $\theta$  has been established for dinuclear complexes, the crossing point between antiferromagnetic and ferromagnetic interactions being located at approximately  $98^\circ$ .<sup>[25a]</sup> DFT calculations carried out on dihydroxo- and dialkoxo-bridged model structures that contain a planar  $\text{Cu}_2(\mu\text{-O}_2)$  skeleton predicted antiferromagnetic interactions for Cu–O–Cu angles ( $\theta$ ) larger than  $92^\circ$  when the  $\tau$  angle (out-of-plane displacement of the carbon atom bonded to the oxygen bridging atom from the  $\text{Cu}_2\text{O}_2$  plane) was zero. Dihydroxo and dialkoxo complexes exhibited antiferromagnetic interactions for the whole range of the Cu–O–Cu angle ( $\theta$ ) when the  $\tau$  angles were smaller than  $40^\circ$ .<sup>[26c,26d]</sup> Moreover, a correlation was established between  $\theta$  and  $\tau$ , which showed that small values of  $\theta$  are associated with the largest values of  $\tau$ . Therefore, the AF coupling is favored when  $\theta$  increases and  $\tau$  diminishes.

The calculated and experimental  $J'$  and  $J''$  values for **1** and **2**, as well as the difference between them, can be justified on the basis of the above magneto-structural correlations and the overlap between the magnetic orbitals along the magnetic exchange pathways. Within the  $\text{Cu}_4\text{O}_4$  cubane unit, each  $\text{Cu}(\text{O})_2\text{Cu}$  bridging fragment with short  $\text{Cu}\cdots\text{Cu}$  distances in the ranges 3.114–3.174 and 3.058–3.174 Å for **1** and **2**, respectively, exhibits two different Cu–O–Cu bridges: one that connects equatorial positions on the neighboring square-pyramidal copper(II) atoms with Cu–O distances of approximately 1.95 Å, and the other one linking equatorial and apical positions on neighboring copper(II) atoms, with  $\text{Cu-O}_{\text{apical}}$  distances in the ranges 2.401–2.506 and 2.282–2.600 Å, for **1** and **2**, respectively (see dotted lines in Figure 4). The latter type of Cu–O–Cu bridge involves one apical position on the square-pyramidal coordination sphere of the copper atom, in which the density of the unpaired electron is very small (the unpaired electron is located in the  $d_{x^2-y^2}$  orbital, which lies in the basal plane and is directed toward the ligand atoms coordinated to the

copper atom). This disposition of the Cu–O–Cu bridge leads to a very small overlap between the magnetic orbitals and, consequently, very weak ferromagnetic or antiferromagnetic interactions are experimentally observed. Therefore, only the equatorial–equatorial Cu–O–Cu bridge will be operative in transmitting the exchange interaction, with its sign and magnitude mainly depending on the  $\theta$  and  $\tau$  angles. These short Cu–O–Cu exchange pathways have  $\theta$  angles in the ranges  $105.45\text{--}107.92^\circ$  (average value  $106.81^\circ$ ) and  $101.20\text{--}109.50^\circ$  (average value  $105.4^\circ$ ) and average  $\tau$  angles of  $45.4$  and  $46.3^\circ$  for **1** and **2**, respectively. Although the experimental magneto-structural correlations for dialkoxo-bridged dinuclear copper(II) complexes<sup>[25]</sup> predict weak to medium antiferromagnetic interactions for the  $\theta$  and  $\tau$  angles observed for **1** and **2** (the effects of  $\theta$  and  $\tau$  are not complementary as the large  $\theta$  values favor antiferromagnetic interactions, whereas the large  $\tau$  values favor ferromagnetic interactions); however, the calculated and experimental  $J_1$  values, as indicated above, are ferromagnetic. As was shown by Alvarez et al. from DFT calculations,<sup>[6a]</sup> this discrepancy can be explained by the presence of chelate ligands attached to the alkoxo bridge, which could introduce an additional exchange pathway between the copper(II) atoms. These additional pathways would ultimately be responsible for the overall ferromagnetic interactions observed for **1** and **2**.

The calculated  $J_1\text{--}J_6$  coupling constants for **1** and **2** (see Scheme 2) are in line with that predicted for the above magneto-structural correlations. For **1**, the larger  $J$  values correspond to the short exchange pathways  $\text{Cu1-O2-Cu2}$  and  $\text{Cu1-O5-Cu3}$ , which are described by  $J_1$  and  $J_2$ , respectively, and have the smaller  $\theta$  ( $105.45$  and  $106.10^\circ$ , respectively) and larger  $\tau$  ( $46.1$  and  $45.01^\circ$ , respectively) angles. The short exchange pathways  $\text{Cu3-O7-Cu4}$  and  $\text{Cu2-O4-Cu4}$ , which are described by  $J_6$  and  $J_5$ , respectively, have larger  $\theta$  ( $107.80$  and  $107.92^\circ$ , respectively) and smaller  $\tau$  angles ( $44.16$  and  $44.99^\circ$ , respectively) than the exchange pathways described by  $J_1$  and  $J_2$ . The increase in  $\theta$  and the decrease in  $\tau$  favor the antiferromagnetic contribution to the magnetic coupling, thus reducing the global ferromagnetic interaction (mean  $J$  value of  $37.05 \text{ cm}^{-1}$  for the ex-

change pathways described by  $J_1$  and  $J_2$  and  $23.4\text{ cm}^{-1}$  for those described by  $J_6$  and  $J_5$ ). In the case of **2**, the larger  $J$  values are found for the short Cu1–O5–Cu3 and Cu3–O7–Cu4 exchange pathways, which are described by  $J_2$  and  $J_6$ , respectively, and characterized by the smaller  $\theta$  ( $102.46$  and  $101.23^\circ$ ) and larger  $\tau$  angles ( $51.5$  and  $49.3^\circ$ ). The other two short exchange pathways in **2**, Cu1–O2–Cu2 and Cu2–O4–Cu4, which are described by  $J_1$  and  $J_5$ , respectively, have larger  $\theta$  ( $109.5$  and  $108.42^\circ$ , respectively) and smaller  $\tau$  angles ( $40.1$  and  $44.5^\circ$ , respectively) than the Cu1–O5–Cu3 and Cu3–O7–Cu4 exchange pathways and consequently exhibit smaller  $J$  values (mean  $J$  value of  $50.95\text{ cm}^{-1}$  for the exchange pathways described by  $J_2$  and  $J_6$  and  $21.05\text{ cm}^{-1}$  for those described by  $J_1$  and  $J_5$ ). The difference between the two couples of mean  $J$  values corresponding to the short Cu–O–Cu exchange pathways in **1** and **2** are bigger for the latter ( $29.9\text{ cm}^{-1}$  vs.  $13.6\text{ cm}^{-1}$ ) because it also exhibits a larger difference between the corresponding mean values of the  $\theta$  angle ( $108.96$  and  $101.84^\circ$  for **2** and  $105.77$  and  $107.86^\circ$  for **1**).

The Cu(O)<sub>2</sub>Cu bridging fragments with long Cu...Cu distances (Cu2–O4–Cu3 and Cu1–O7–Cu4) contain two equatorial-axial bridges and therefore weak ferromagnetic or antiferromagnetic interactions little dependent on the geometrical factors, are expected. The experimental and calculated weak ferromagnetic interactions extracted for **1** and **2** agree with this prediction and match well in sign and magnitude with those calculated by other authors.<sup>[6a]</sup>

It is worth noting that the ligands used for preparing **1** and **2** are very similar, with both being NO<sub>2</sub> tridentate chelate bridging Schiff bases. Therefore, the differences between the  $J'$  values observed for **1** and **2** should mainly arise from their differences in  $\theta$  and  $\tau$  angles rather than to

differences in the Schiff base ligands. Thus, complex **2**, which shows smaller  $\theta$  and bigger  $\tau$  values than **1**, presents a larger  $J'$  value, as expected from the experimental and calculated magneto-structural correlation for alkoxo-bridged dinuclear copper(II) complexes.<sup>[6a,25,26]</sup>

The spin-density distribution for **1** and **2** (the spin density of **1** is given as an example in Figure 5, whereas that of **2** is given in the Supporting Information) clearly shows that the spin density of the copper(II) atoms has the shape of a  $d_{x^2-y^2}$  orbital and it is  $\sigma$  delocalized on the donor atoms directly attached to the metal. As expected, the delocalization is more important for the atoms directly bound to the Cu<sup>II</sup> atoms. Moreover, the spin density is mainly found at the metal, as expected if they are the magnetic centres (see Table 4).

Table 4. Selected values of the spin density for complexes **1** and **2**.

	<b>1</b>	<b>2</b>
Cu1	0.6222	0.6311
Cu2	0.6273	0.6254
Cu3	0.6327	0.6306
Cu4	0.6256	0.6193
O1 <sub>alcoholate</sub> <sup>[a]</sup>	0.1570	0.1757
O2 <sub>alcoholate</sub>	0.1620	0.1540
O3 <sub>alcoholate</sub>	0.1564	0.1655
O4 <sub>alcoholate</sub>	0.1600	0.1568
O1 <sub>phenolate</sub>	0.0919	0.0979
O2 <sub>phenolate</sub>	0.0931	0.0938
O3 <sub>phenolate</sub>	0.0974	0.0958
O4 <sub>phenolate</sub>	0.0930	0.0967
N1	0.1104	0.1064
N2	0.1091	0.1077
N3	0.1116	0.1070
N4	0.1133	0.1118

[a] The labels 1–4 for oxygen and nitrogen refer to the atom that belongs to the ligand coordinating the corresponding copper atom (1–4).

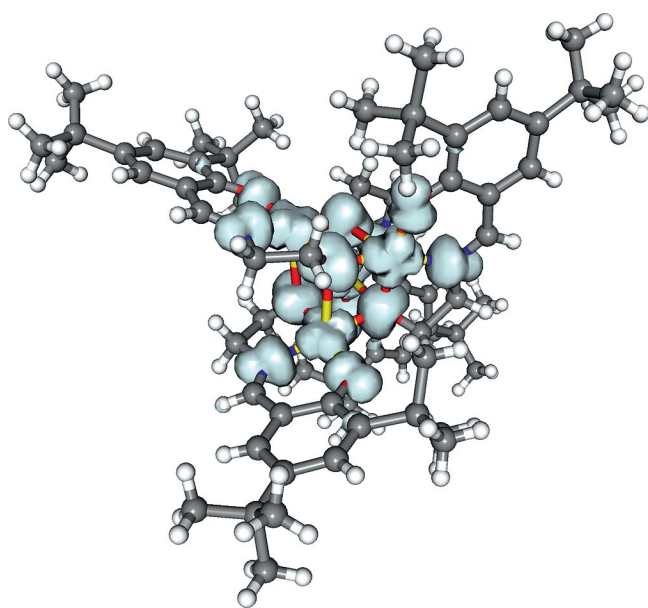


Figure 5. View of the calculated spin-density distribution for the quintuplet state of **1**. Gray shapes correspond to positive spin densities. The isodensity surface corresponds to a cutoff value of  $0.0015\text{ e bohr}^{-3}$ .

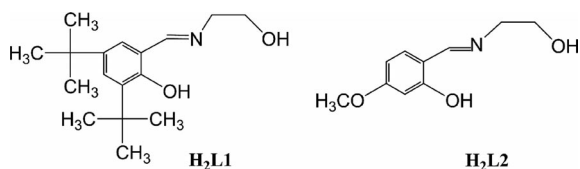
## Conclusion

Two new Cu<sub>4</sub>O<sub>4</sub> cubane-like complexes were prepared from two closely related NO<sub>2</sub> chelate tridentate bridging Schiff base ligands. Experimental magnetic studies showed that complexes **1** and **2** exhibit dominant ferromagnetic coupling. Complexes **1** and **2** exhibit a rather distorted open cubane-like Cu<sub>4</sub>O<sub>4</sub> structure with four short and two long Cu...Cu distances and therefore belong to the 4+2 type. Although six different  $J$  values should be taken into account to analyze the magnetic data, we have assumed that the exchange coupling constants between the copper(II) ions that involve short Cu...Cu distances are equivalent and described by  $J'$ , whereas those which involve long Cu...Cu distances are described by  $J''$ . The values of the magnetic exchange coupling constant extracted from the experimental susceptibility data were as follows:  $J' = +28.7\text{ cm}^{-1}$ ,  $J'' = +7.8\text{ cm}^{-1}$  for **1**, and  $J' = +39.8\text{ cm}^{-1}$ ,  $J'' = +10.2\text{ cm}^{-1}$  for **2**. DFT calculations on the structures of **1** and **2** as found in the solid state afforded  $J$  values that agree well with the experimental ones. Moreover, the six calculated  $J$

coupling constants for the  $\text{Cu}_4\text{O}_4$  unit in **1** and **2** follow the trend predicted by the magneto-structural correlations previously established for dialkoxo-bridged dicopper(II) complexes (the ferromagnetic interaction decreases with the increase in the Cu–O–Cu bridging angle ( $\theta$ ) and with the decrease in the  $\tau$  angle that describes the out-of-plane displacement of the carbon atom bonded to the oxygen bridging atom from the  $\text{Cu}_2\text{O}_2$  plane). To the best of our knowledge, complexes **1** and **2** are the first examples of 4+2  $\text{Cu}_4\text{O}_4$  complexes in which both coupling constants ( $J'$  and  $J''$ ) are ferromagnetic, and thus in good agreement with previous DFT calculations that predicted a positive sign for  $J''$ .

## Experimental Section

**Physical Measurements:** All chemical reagents and solvents were purchased from Merck or Aldrich and used without further purification. Elemental (C, H, N) analyses were carried out by standard methods with a LECO, CHNS-932 analyzer. FTIR spectra were measured with a Perkin–Elmer Model Bx 1600 instrument with the samples as KBr pellets in the 4000–400  $\text{cm}^{-1}$  range. The temperature dependence of the magnetic susceptibility of polycrystalline samples was measured between 2 and 300 K at a field of 1.0 T using a Quantum Design model MPMS computer-controlled SQUID magnetometer. The synthetic route of the ligand and complexes are outlined in Scheme 3.



Scheme 3. The ligands  $\text{H}_2\text{L1}$  and  $\text{H}_2\text{L2}$  used in this study.

**Synthesis of  $\text{H}_2\text{L1}$  and  $\text{H}_2\text{L2}$  Ligands:** The tridentate Schiff base ligand  $\text{H}_2\text{L1}$  was synthesized from 3,5-di-*tert*-butyl-2-hydroxybenzaldehyde and ethanolamine in a 1:1 molar ratio in hot methanol according to the method reported previously.<sup>[8]</sup>  $\text{H}_2\text{L2}$  was prepared in a similar way by using 2-hydroxy-4-methoxybenzaldehyde in hot methanol. The ligands  $\text{H}_2\text{L1}$  and  $\text{H}_2\text{L2}$  evaluated in this study are outlined in Scheme 3. For  $\text{H}_2\text{L1}$ : Yellow crystals, yield 80%.  $\text{C}_{17}\text{H}_{27}\text{O}_2\text{N}$  (277.40): calcd. C 73.60, H 9.81, N 5.04; found C 72.25, H 9.02, N 5.12. For  $\text{H}_2\text{L2}$ : Brown crystals, yield 80%.  $\text{C}_{10}\text{H}_{13}\text{O}_3\text{N}$  (195.21): calcd. C 61.52, H 6.71, N 7.17; found C 60.23, H 6.17, N 6.98.

**Synthesis of Complex **1** and **2**:** Complexes **1** and **2** were prepared by the addition of copper(II) acetate monohydrate (0.199 g, 1 mmol) in hot methanol (20  $\text{cm}^3$ ) to the appropriate ligand ( $\text{H}_2\text{L1}$  and  $\text{H}_2\text{L2}$ ) (1 mmol) in hot methanol (30  $\text{cm}^3$ ). Triethylamine ( $\text{Et}_3\text{N}$ ; 1 mmol) was then added to the resulting solution. The mixture was warmed to 65 °C and stirred for 15 min. A green solution was obtained, which was allowed to stand at room temperature for several weeks to afford green crystals. Complex **1**: Green crystals, yield 75%.  $\text{C}_{68}\text{H}_{100}\text{Cu}_4\text{N}_4\text{O}_8$  (1355.68): calcd. C 60.24, H 7.43, N 4.13; found C 60.20, H 7.52, N 4.18. IR (KBr):  $\tilde{\nu}$  = 3306, 2956, 2870, 2380, 1645, 1449, 1115, 535, 475  $\text{cm}^{-1}$ . Complex **2**: Green crystals, yield 75%.  $\text{C}_{40}\text{H}_{44}\text{Cu}_4\text{N}_4\text{O}_{12}$  (1026.95): calcd. C 46.78, H 4.32, N 5.46; found C 46.12, H 4.34, N 5.10. IR (KBr):  $\tilde{\nu}$  = 3053, 2922, 2830, 2361, 1648, 1595, 1240, 579, 485  $\text{cm}^{-1}$ .

**X-ray Structural Determination:** Diffraction measurements were carried out with an Oxford Diffraction Xcalibur3 diffractometer at 293 K for **1** and with a Bruker Apex II Kappa CCD diffractometer at 100 K for **2** by using graphite-monochromated Mo- $K_\alpha$  radiation ( $\lambda = 0.71073 \text{ \AA}$ ). The intensity data were integrated using the AP-EXII program.<sup>[9]</sup> Absorption corrections were applied on the basis of equivalent reflections using SADABS.<sup>[10]</sup> The structures were solved by direct methods and refined using full-matrix least-squares against  $F^2$  using SHELXL.<sup>[11]</sup> All non-hydrogen atoms were assigned anisotropic displacement parameters and refined without positional constraints. Hydrogen atoms were included in idealized positions with isotropic displacement parameters constrained to 1.5 times the  $U_{\text{equiv}}$  of their attached carbon atoms for methyl hydrogen atoms, and 1.2 times the  $U_{\text{equiv}}$  of their attached carbon atoms for all others. A possible disorder in the ethanolamine portion of the ligand and one methoxy group of **1** has been considered. However, the nineteen carbon atoms of methoxy groups were refined isotropically owing to their high thermal motion.

Powder X-ray measurements were performed using Cu- $K_\alpha$  radiation ( $\lambda = 1.5418 \text{ \AA}$ ) with a Bruker-AXS D8-Avance diffractometer equipped with a secondary monochromator. The data were collected in the range  $5^\circ < 2\theta < 50^\circ$  in  $\theta$ - $\theta$  mode with a step time of  $n$  s ( $5 \text{ s} < n < 10 \text{ s}$ ) and a step width of 0.03°.

**Computational Details:** All theoretical calculations were carried out at the DFT level of theory using the hybrid B3LYP exchange-correlation functional,<sup>[12–14]</sup> as implemented in the Gaussian 03 program.<sup>[15]</sup> A quadratic convergence method was employed in the self-consistent field (SCF) process.<sup>[16]</sup> The triple- $\xi$  quality basis set proposed by Ahlrichs and co-workers has been used for all atoms.<sup>[17]</sup> Calculations were performed on the complexes built from the experimental geometries. The electronic configurations used as starting points were created using the Jaguar 7.6 software.<sup>[18]</sup> The approach used to determine the exchange coupling constants for polynuclear complexes has been described in detail elsewhere.<sup>[19–22]</sup> To calculate  $nJ_i$  exchange coupling constants of a polynuclear complex, we must perform at least  $n + 1$  energy calculations of different spin configurations that correspond to single-determinant Kohn–Sham solutions.<sup>[21]</sup> Therefore, seven calculations are necessary for complex **1** to obtain the values of five exchange coupling constants (see Table 3). However, additional electronic configurations have been calculated to verify possible errors or shortcomings in the computational procedure. The values of the  $J_i$  constants were obtained by a fit-process from the energy found for the chosen spin configurations.

CCDC-826612 (for **1**) and -826610 (for **2**) contain the supplementary crystallographic data for this paper. These data can be obtained free of charge from The Cambridge Crystallographic Data Centre via [www.ccdc.cam.ac.uk/data\\_request/cif](http://www.ccdc.cam.ac.uk/data_request/cif).

**Supporting Information** (see footnote on the first page of this article): Powder XRD patterns for **1** and **2**, and view of the calculated spin-density distribution for the quintuplet state of **2**. Also includes the relationships derived from the difference between the energy of the HS state and that of the BS states, from which the  $J_i$  parameters can be calculated, and the spin-density distribution for complex **2**.

## Acknowledgments

The authors are grateful to the Research Funds of Balikesir University (grant number BAP-2010/33) and The Scientific and Technological Research Council of Turkey (TUBITAK) (grant number TBAG-108T431) for the financial support. H. K. thanks the Nato-

BL-TUBITAK for funding and Prof. Guy Orpen (School of Chemistry, University of Bristol, UK) for his hospitality. The authors are also very grateful to Dr. Yasemin Yahsi (The University of Balikesir) for the X-ray measurement, and Dr. Lorenzo Sorace and Dr. Andrea Caneschi (Department of Chemistry, University of Florence) for SQUID measurements. E. C. and A. M. offer their thanks to the Spanish Ministerio de Economía y Competitividad (MINECO) (project number CTQ-2011-24478/BQU), the Junta de Andalucía, and the University of Granada for financial support. The authors would also like to thank the Centro de Supercomputación de la Universidad de Granada for computational resources.

- [1] a) G. R. Newkome, E. He, C. N. Moorefield, *Chem. Rev.* **1999**, *99*, 1689–1746; b) S. Leininger, B. Olenyuk, P. J. Stang, *Chem. Rev.* **2000**, *100*, 853–907; c) J. Y. Lu, *Coord. Chem. Rev.* **2003**, *246*, 327–347; d) A. Y. Robin, K. M. Fromm, *Coord. Chem. Rev.* **2006**, *250*, 2127–2157; e) C. J. Adams, M. A. Kurawa, M. Lusi, A. G. Orpen, *CrystEngComm* **2008**, *10*, 1790–1795; f) M. Chang, M. Chung, B. S. Lee, C. H. Kwak, *J. Nanosci. Nanotechnol.* **2006**, *6*, 3338–3342; g) S. G. Kang, H. Kim, S. Bang, *Inorg. Chim. Acta* **2013**, *396*, 10–13.
- [2] a) O. Kahn, *Molecular Magnetism*, VCH Publishers, New York, **1993**; b) O. Kahn, *Acc. Chem. Res.* **2000**, *33*, 647–657; c) E. Coronado, P. Day, *Chem. Rev.* **2004**, *104*, 5419–5448; d) Z. Lu, T. Fan, W. Guo, J. Lu, C. Fan, *Inorg. Chim. Acta* **2013**, *400*, 191–196; e) C. M. Liu, R. G. Xiong, D. Q. Zhang, D. B. Zhu, *J. Am. Chem. Soc.* **2010**, *132*, 4044–4045; f) G. Karotsis, S. Kenedy, S. J. Teat, C. M. Beavers, D. A. Fowler, J. J. Morales, M. Evangelisti, S. J. Dalgarno, E. K. Brechin, *J. Am. Chem. Soc.* **2010**, *132*, 12983–12990; g) J. Zhang, P. Teo, R. Pattacini, A. Kermagoret, R. Welter, G. Rogez, T. S. A. Hor, P. Braunstein, *Angew. Chem.* **2010**, *122*, 4545; *Angew. Chem. Int. Ed.* **2010**, *49*, 4443–4446; h) E. Gungor, H. Kara, *Inorg. Chim. Acta* **2012**, *384*, 137–142; i) M. F. Haddow, H. Kara, G. R. Owen, *Inorg. Chim. Acta* **2009**, *362*, 3502–3506; j) Y. Elerman, H. Kara, A. Z. Elmali, *Naturforsch. Teil A* **2003**, *58*, 363–372.
- [3] a) R. Huber, *Angew. Chem.* **1989**, *101*, 849; *Angew. Chem. Int. Ed. Engl.* **1989**, *28*, 848–869; b) E. I. Solomon, U. M. Sundaram, T. E. Machonkin, *Chem. Rev.* **1996**, *96*, 2563–2606; c) P. Gamez, P. G. Aubel, W. L. Driessen, J. Reedijk, *Chem. Soc. Rev.* **2001**, *30*, 376–385; d) E. I. Solomon, R. K. Szilagyi, S. DeBeer George, L. Basumallick, *Chem. Rev.* **2004**, *104*, 419–458; e) G. Henkel, B. Krebs, *Chem. Rev.* **2004**, *104*, 801–824; f) Y. Zhao, T. Gong, Z. Yu, S. Zhu, W. He, T. Ni, Z. Guo, *Inorg. Chim. Acta* **2013**, *399*, 112–118; g) L. Tjioe, A. Meininger, T. Joshi, L. Spiccia, B. Graham, *Inorg. Chem.* **2011**, *50*, 4327–4339; h) S. S. Bhat, A. A. Kumbhar, H. Heptullah, A. A. Khan, V. V. Gobre, S. P. Gejji, V. G. Puranik, *Inorg. Chem.* **2011**, *50*, 545–558.
- [4] a) R. Wegner, M. Gottschaldt, H. Görls, E. Jäger, D. Klemm, *Chem. Eur. J.* **2001**, *7*, 2143–2157; b) M. M. Diaz-Requejo, P. J. Pérez, *Chem. Rev.* **2008**, *108*, 3379–3394; c) A. M. Kirillov, M. V. Kirillova, A. J. L. Pombeiro, *Coord. Chem. Rev.* **2012**, *256*, 2741–2759; d) S. Löw, J. Becker, C. Würtele, A. Miska, C. Kleeberg, U. Behrens, O. Walter, S. Schindler, *Chem. Eur. J.* **2013**, *19*, 5342–5351; e) E. Safaei, A. Wojtczak, E. Bill, H. Hamidi, *Polyhedron* **2010**, *29*, 2769–2775; f) E. Safaei, M. M. Kabir, A. Wojtczak, Z. Jaglicic, A. Kozakiewicz, Y. I. Lee, *Inorg. Chim. Acta* **2011**, *366*, 275–282.
- [5] a) H. H. Monfared, J. Sanchiz, Z. Kalantari, C. Janiak, *Inorg. Chim. Acta* **2009**, *362*, 3791–3795; b) J. W. Lu, Y. H. Huang, S. Lo, H. H. Wei, *Inorg. Chem. Commun.* **2007**, *10*, 1210–1213; c) X. S. Tan, Y. Fujii, R. Nukada, M. Mikuriyaand, Y. Nakano, *J. Chem. Soc., Dalton Trans.* **1999**, 2415–2416; d) X. F. Yan, J. Pan, S. R. Li, H. Zhou, Z. Q. Pan, *Z. Anorg. Allg. Chem.* **2009**, *635*, 1481–1484; e) A. Burkhardt, E. T. Spielberg, H. Görls, W. Plass, *Inorg. Chem.* **2008**, *47*, 2485–2493; f) Y. Xie, H. Jiang, A. S.-C. Chan, Q. Liu, X. Xu, C. Dud, Y. Zhu, *Inorg. Chim. Acta* **2002**, *333*, 138–143; g) V. T. Yilmaz, V. Kars, C. Kazak, *Z. Anorg. Allg. Chem.* **2007**, *633*, 351–353; h) C. Maxim, T. D. Pasatoiu, V. C. Kravtsov, S. Shova, C. A. Muryn, R. E. P. Wippeny, F. Tuna, M. Andruh, *Inorg. Chim. Acta* **2008**, *361*, 3903–3911; i) L. Merz, W. Haase, *J. Chem. Soc., Dalton Trans.* **1978**, *11*, 1594–1598; j) R. Mergehenn, L. Merz, W. Haase, *J. Chem. Soc., Dalton Trans.* **1980**, *17*, 1703–1709; k) M. Nihei, N. Hoshino, T. Ito, H. Oshio, *Polyhedron* **2003**, *22*, 2359–2362; l) H. Oshio, Y. Saito, T. Ito, *Angew. Chem.* **1997**, *109*, 2789–2791; m) H. Oshio, Y. Saito, T. Ito, *Angew. Chem.* **1997**, *109*, 2789; *Angew. Chem. Int. Ed. Engl.* **1997**, *36*, 2673–2675; n) L. Walz, H. Paulus, W. Haase, *J. Chem. Soc., Dalton Trans.* **1983**, 657–664; o) Y. M. Li, J. J. Zhang, R. B. Fu, S. C. Xiang, T. L. Sheng, D. Q. Yuan, X. H. Huang, X. T. Wu, *Polyhedron* **2006**, *25*, 1618–1624; p) L. Schwabe, W. Haase, *J. Chem. Soc., Dalton Trans.* **1985**, 1909–1913; q) N. Matsumoto, I. Ueda, Y. Nishida, S. Kida, *Bull. Chem. Soc. Jpn.* **1976**, *49*, 1308–1312; r) A. Mukherjee, R. Raghunathan, M. K. Saha, M. Nethaji, S. Ramasesha, A. R. Chakravarty, *Chem. Eur. J.* **2005**, *11*, 3087–3096; s) H. Astheimer, F. Nepveu, L. Walz, W. Haase, *J. Chem. Soc., Dalton Trans.* **1985**, 315–320; t) R. Wegner, M. Gottschaldt, H. Görls, E. G. Jäger, D. Klemm, *Chem. Eur. J.* **2001**, *7*, 2143–2157; u) J. Chakraborty, S. Thakurta, G. Pilet, D. Luneau, S. Mitra, *Polyhedron* **2009**, *28*, 819–825; v) E. A. Buvaylo, V. N. Kokozyay, O. Y. Vassilyeva, B. W. Skelton, J. Jezierska, L. C. Bruneland, A. Ozarowski, *Inorg. Chem.* **2005**, *44*, 206–216; w) M. L. Liu, J. M. Dou, J. Z. Cui, D. C. Li, D. Q. Wang, *J. Mol. Struct.* **2012**, *1011*, 140–144.
- [6] a) E. Ruiz, S. Alvarez, A. Rodríguez-Forteza, P. Alemany, *J. Mater. Chem.* **2006**, *16*, 2729–2735; b) E. Ruiz, S. Alvarez, A. Rodríguez-Forteza, P. Alemany, Y. Pouillon, C. Massobrio, J. S. Miller, M. Drillon Eds (Eds.), *Electronic Structure and Magnetic Behavior in Polynuclear Transition-Metal Compounds*, vol. 2, Wiley-VCH, Weinheim, Germany, **2001**; c) E. Ruiz, A. Rodríguez-Forteza, P. Alemany, S. Alvarez, *Polyhedron* **2001**, *20*, 1323–1327.
- [7] R. Mergehenn, W. Haase, *Acta Crystallogr., Sect. B* **1977**, *33*, 1877–1882.
- [8] S. Jammi, T. Punniyamurth, *Eur. J. Inorg. Chem.* **2009**, 2508–2511.
- [9] *SAINT*, v. 760A, Bruker-AXS, Inc., Madison, Wisconsin, USA, **2002**.
- [10] G. M. Sheldrick, *SADABS*, v. 2008/1, University of Göttingen, Germany, **2003**.
- [11] G. Sheldrick, *Acta Crystallogr., Sect. A* **2008**, *64*, 112–122.
- [12] A. D. Becke, *Phys. Rev. A* **1988**, *38*, 3098–3100.
- [13] C. Lee, W. Yang, R. G. Parr, *Phys. Rev. B* **1988**, *37*, 785–789.
- [14] A. D. Becke, *J. Chem. Phys.* **1993**, *98*, 5648–5652.
- [15] M. J. Frisch, G. W. Trucks, H. B. Schlegel, G. E. Scuseria, M. A. Robb, J. R. Cheeseman, J. J. A. Montgomery, T. Vreven, K. N. Kudin, J. C. Burant, J. M. Millam, S. S. Iyengar, J. Tomasi, V. Barone, B. Mennucci, M. Cossi, G. Scalmani, N. Rega, G. A. Petersson, H. Nakatsuji, M. Hada, M. Ehara, K. Toyota, R. Fukuda, J. Hasegawa, M. Ishida, T. Nakajima, Y. Honda, O. Kitao, H. Nakai, M. Klene, X. Li, J. E. Knox, H. P. Hratchian, J. B. Cross, V. Bakken, C. Adamo, J. Jaramillo, R. Gomperts, R. E. Stratmann, O. Yazyev, A. J. Austin, R. Cammi, C. Pomelli, J. W. Ochterski, P. Y. Ayala, K. Morokuma, G. A. Voth, P. Salvador, J. J. Dannenberg, V. G. Zakrzewski, S. Dapprich, A. D. Daniels, M. C. Strain, O. Farkas, D. K. Malick, A. D. Rabuck, K. Raghavachari, J. B. Foresman, J. V. Ortiz, Q. Cui, A. G. Baboul, S. Clifford, J. Cioslowski, B. B. Stefanov, G. Liu, A. Liashenko, P. Piskorz, I. Komaromi, R. L. Martin, D. J. Fox, T. Keith, M. A. Al-Laham, C. Y. Peng, A. Nanayakkara, M. Challacombe, P. M. W. Gill, B. Johnson, W. Chen, M. W. Wong, C. Gonzalez, J. A. Pople, *Gaussian 03*, revision C02, Gaussian Inc, Wallingford CT, **2004**.
- [16] G. B. Bacskay, *Chem. Phys.* **1981**, *61*, 385–404.
- [17] A. Schäfer, C. Huber, R. Ahlrichs, *J. Chem. Phys.* **1994**, *100*, 5829–5835.
- [18] *Jaguar 76*, Schrödinger, Inc., Portland OR, **2009**.

- [19] E. Ruiz, J. Cano, S. Alvarez, P. Alemany, *J. Comput. Chem.* **1999**, *20*, 1391–1400.
- [20] E. Ruiz, S. Alvarez, A. Rodríguez-Forteza, P. Alemany, Y. Pouillon, C. Massobrio, *Magn. Mol. Mater. II* **2001**, 227–279.
- [21] E. Ruiz, A. Rodríguez-Forteza, J. Cano, S. Alvarez, P. Alemany, *J. Comput. Chem.* **2003**, *24*, 982–989.
- [22] E. Ruiz, S. Alvarez, J. Cano, V. Polo, *J. Chem. Phys.* **2005**, *123*, 164110/1–164140/7.
- [23] A. W. Addison, T. N. Rao, J. Reedijk, J. Van Rijn, G. C. Verschoor, *J. Chem. Soc., Dalton Trans.* **1984**, 1349–1356.
- [24] J. J. Borrás-Almenar, J. M. Clemente-Juan, E. Coronado, B. S. Tsukerblat, *J. Comput. Chem.* **2001**, *22*, 985–991.
- [25] a) V. H. Crawford, H. W. Richardson, J. R. Wasson, D. J. Hodgson, W. E. Hatfield, *Inorg. Chem.* **1976**, *15*, 2107–2110; b) L. Merz, W. Haase, *J. Chem. Soc., Dalton Trans.* **1980**, 875–879; c) L. Walz, H. Paulus, W. Haase, *J. Chem. Soc., Dalton Trans.* **1985**, 913–920; d) L. Walz, W. Haase, *J. Chem. Soc., Dalton Trans.* **1985**, 1243–1248; e) T. Lindgren, R. Sillanpää, K. Rissanen, L. K. Thompson, C. J. O'Connor, G. A. Van Albada, J. Reedijk, *Inorg. Chim. Acta* **1990**, *171*, 95–102; f) A. M. Kirillov, Y. Y. Karabach, M. Haukka, M. F. C. Guedes da Silva, J. Sanchiz, M. N. Kopylovich, A. J. L. Pombeiro, *Inorg. Chem.* **2008**, *47*, 162–175; g) L. J. Farrugia, D. S. Middlemiss, R. Sillanpää, P. Seppälä, *J. Phys. Chem. A* **2008**, *112*, 9050–967; h) P. Seppälä, E. Colacio, A. J. Mota, R. Sillanpää, *Inorg. Chim. Acta* **2010**, *363*, 755–762; i) P. Seppälä, E. Colacio, A. J. Mota, R. Sillanpää, *Dalton Trans.* **2012**, *41*, 2648–2658.
- [26] See, for example: a) H. Astheimer, W. Haase, *J. Chem. Phys.* **1986**, *85*, 1427–1432; b) M. Handa, N. Koga, S. Kida, *Bull. Chem. Soc. Jpn.* **1988**, *61*, 3853–3857; c) E. Ruiz, P. Alemany, S. Alvarez, J. Cano, *J. Am. Chem. Soc.* **1997**, *119*, 1297–1303; d) E. Ruiz, P. Alemany, S. Alvarez, J. Cano, *Inorg. Chem.* **1997**, *36*, 3683–3688; e) H. Hu, D. Zhang, Z. Chen, C. Liu, *Chem. Phys. Lett.* **2000**, *329*, 255–260; f) H. Hu, Y. Liu, D. Zhang, C. Liu, *THEOCHEM* **2001**, *546*, 73–78; g) H. Hu, X. Yang, Z. Chen, *THEOCHEM* **2002**, *618*, 41–46; h) A. Rodríguez-Forteza, E. Ruiz, P. Alemany, S. Alvarez, *Monatsh. Chem.* **2003**, *134*, 307–316; i) C. J. Calzado, D. Maynau, *J. Chem. Phys.* **2011**, *135*, 194704.

Received: December 2, 2013

Published Online: February 24, 2014